Microbial regulation of intestinal radiosensitivity

Peter A. Crawford and Jeffrey I. Gordon*

Center for Genome Sciences and Departments of Molecular Biology and Pharmacology and Medicine, Washington University School of Medicine,
St. Louis, MO 63108

We describe a method for treating germ-free (GF) mice with γ-irradiation and transplanting them with normal or genetically manipulated bone marrow while maintaining their GF status. This approach revealed that GF mice are markedly resistant to lethal radiation enteritis. Furthermore, administering lethal doses of total body irradiation to GF mice produces markedly fewer apoptotic endothelial cells and lymphocytes in the mesenchymal cores of their small intestinal villi, compared with conventionally raised animals that have acquired a microbiota from birth. Analysis of GF and conventionally raised $Rag1^{-/-}$ mice disclosed that mature lymphocytes are not required for the development of lethal radiation enteritis or the microbiota-associated enhancement of endothelial radiosensitivity. Studies of gnotobiotic knockout mice that lack fasting-induced adipose factor (Fiaf), a fibrinogen/angiopoietin-like protein normally secreted from the small intestinal villus epithelium and suppressed by the microbiota, showed that Fiaf deficiency results in loss of resistance of villus endothelial and lymphocyte populations to radiation-induced apoptosis. Together, these findings provide insights about the cellular and molecular targets involved in microbial regulation of intestinal radiosensitivity.

endothelial cell apoptosis | fasting-induced adipose factor | gnotobiotic knockout and radiation chimeric mice | gut microbiota | radiation enteritis

The adult human intestine is colonized by 10 trillion to 100 trillion microbes. This microbiota is dominated by members of Bacteria but also contains representatives of Archaea and Eukarya. The extent of diversity in this community is not well defined within or between individuals, although the most comprehensive 16S rRNA-based enumeration of colonic mucosal and fecal microbial communities published to date, involving a small number of healthy adults, yielded 395 operational taxonomic units representing 8 bacterial divisions (superkingdoms), with the Bacteroidetes and Firmicutes divisions predominating (1, 2). These gut microbes and their genomes (the microbiome) endow us with physiologic capacities that we have not had to evolve on our own and thus are both a manifestation of who we are genetically and metabolically and a reflection of our state of well-being.

Insights about how our physiology is shaped by the microbiota have come from comparative studies of germ-free (GF) animals raised in the absence of microbes and conventionally raised (CONV-R) animals that either acquire a microbiota from birth or are initially GF and then colonized at various stages of postnatal life or adulthood with a gut microbiota from CONV-R donors ("conventionalized," CONV-D) (3). These gnotobiotic models have revealed that the microbiota facilitates the breakdown of otherwise indigestible polysaccharide components of our diet (4, 5), regulates storage of calories extracted from the diet in adipocytes (3), metabolizes xenobiotics, including carcinogens (6, 7), modulates intestinal epithelial cell turnover (8–11), and educates the immune system (12, 13). The microbiota also collaborates with the host to regulate a number of aspects of postnatal gut development, including the assembly of the extensive network of capillaries in the mesenchymal cores of mouse small intestinal villi (14).

Understanding the nature of host–microbial mutualism in our gut promises to affect not only how we predict the development of disease but also how we treat diseases. Ionizing radiation is part of the treatment regimens of at least half of all patients with malignancies. The deleterious effects of ionizing radiation on the intestine were first described in 1897, 2 years after the initial discovery of x-rays by Wilhelm Röntgen. Since the early 1900s, radiation enteritis has been thought to be exacerbated by the gut microbiota (15). Antibiotics have been used in human clinical trials to manipulate the radiosensitivity of the intestine, but no clearly effective protocol has emerged to date (16–18).

The responses of GF animals to ionizing radiation were first studied in the late 1950s (19) and differ from those of CONV-R animals in a number of ways. First, the minimum dose required to induce 50% mortality is higher in GF mice (20). Second, after receiving lethal doses of total body irradiation (TBI), GF animals survive longer than their CONV-R counterparts (20–22). Third, the minimum TBI dose that produces histological evidence of radiation enteritis (mucosal atrophy, mesenchymal inflammation, and fibrosis) is higher in GF mice, compared with animals with a microbiota (21). In contrast, the dose threshold and extent of TBI-induced damage to bone marrow are equivalent in GF and CONV-R mice (23, 24).

The authors of these original studies suggested that the enhanced lethality of TBI in CONV-R mice is related to systemic infection and/or greater susceptibility to intestinal damage. However, the precise nature of the cellular damage, its relationship to survival, and the molecular pathways through which the microbiota operates to influence intestinal radiosensitivity remain poorly defined. In this study, we use adult GF, CONV-R, and/or CONV-D normal, knockout, and chimeric mice treated with TBI and bone marrow transplantation (BMT) to show that (*i*) gut microbes affect the radiosensitivity of endothelial cells and lymphocytes populating the mesenchyme of small intestinal villi, and that (*ii*) an epithelial-derived, secreted member of the angiopoietin family whose expression is normally suppressed by the microbiota modulates the radioresistant intestinal phenotype of GF animals.

Materials and Methods

Mice. CONV-R WT FVB/N mice were purchased from Taconic Farms. C57BL/6J (B6) WT, $Rag1^{-/-}$, $iNOS^{-/-}$, and FVB/N *Tie2-GFP* transgenic mice were obtained from The Jackson Laboratory. Male and female FVB/N and B6 WT mice were rederived as GF and conventionalized or were colonized with one or two components of the normal gut microbiota (25). GF and CONV-D $Fiaf^{-/-}$ mice (hybrid C57BL/6J × 129/SvJ background) were produced according to ref. 3. *Sca1-EGFP* knock-in mice (originally on a B6/129 hybrid background but backcrossed to B6 to generation N7) were generously supplied by Timothy Graubert (Washington University).

GF, CONV-D, and specified pathogen-free CONV-R WT and genetically engineered mice were maintained under a 12-h light cycle and given an autoclaved standard rodent chow diet (B&K, Zeigler Brothers, Gardners, PA) plus sterilized tap water ad libitum. GF and CONV-D mice were housed in plastic gnotobiotic isolators (25). All experiments involving mice were performed by using protocols approved by the Washington University Animal Studies Committee.

TBI and BMT of GF Mice. An irradiator pie-plate for housing animals was sterilized with aerosolized chlorine dioxide (Clidox-S, Pharmacal Research Labs, Waterbury, CT) and passed into a flexible film gnotobiotic isolator, where it was fitted with a sterile fiberglass filter top (0.6-cm-thick Afs-4 filter media, Class Biologically Clean, Madison, WI) to allow air, but not microbes, to pass through. GF mice in this container were removed from the isolator and treated in a Mark I ^{137}Cs irradiator (106 cGy/min for a total dose of 10–22 Gy; Shepherd, San Fernando, CA). After irradiation, the container was placed in the gnotobiotic isolator's entry port. After sterilization for 20 min with Clidox-S, the inner door of the port was removed, the container was pulled through, and the port was closed. Mice were then returned to their cages within the isolator.

For transplantation of unfractionated bone marrow, 8- to 12-week-old strain-, gender-, and genotype-matched donor mice were killed and sprayed with 70% ethanol, and their femurs and tibias were recovered by dissection. In a laminar-flow hood, the contents of these long bones were flushed into Hanks' balanced salt solution containing 100 units/ml penicillin and 100 μg/ml streptomycin. Fibrous debris was allowed to settle by gravity, and the cell-enriched supernatant was aspirated and centrifuged (2,000 × g for 10 min at 25°C). The resulting cell pellet was resuspended in 1–2 ml of PBS supplemented with 100 units/ml penicillin and 100 μg/ml streptomycin. Cells were counted (hemocytometer) and aliquots were put into sterile screw-cap tubes. One donor mouse provided cells for three to four recipients: each recipient received ≈5 × 10^6 antibiotic-sterilized cells.

For BMT of GF mice, 1-ml syringes and 30-gauge needles were autoclaved in a transporting cylinder and shuttled into the gnotobiotic isolator through its port. A sterile screw-cap tube, containing rodent anesthesia mixture consisting of ketamine (100 mg/ml), xylazine (20 mg/ml), and acepromazine (10 mg/ml) that had been passed through a 0.2-μm filter, was sterilized in the port of the gnotobiotic isolator and then passed into the isolator. GF mice received an i.p. dose of 0.25 ml of the anesthesia mixture at least 6 h but not >18 h after TBI. The screw-cap tube containing the donor bone marrow cells was passed into the isolator by using the same procedure used for the anesthesia mixture. Once in the isolator, the tube was rinsed in sterile water before cells were collected in a 1-ml syringe and a 100- to 200-μl aliquot was delivered to the recipient via retroorbital injection.

To confirm preservation of the GF state after TBI–BMT, fecal samples from mice in the isolators were cultured in brain–heart infusion broth, Sabouraud dextrose broth, and nutrient broth, all from VWR Scientific, at 37°C and 42°C under aerobic and anaerobic conditions. Spleens were dissected from mice by using sterile techniques, homogenized in 1 ml of PBS, and serial dilutions (in PBS) were plated on brain–heart infusion blood agar. The plates were subsequently cultured under aerobic and anaerobic conditions.

Statistics. Log-rank analysis was used to compare survival curve data. The significance of observed differences in intestinal mesenchymal apoptosis among members of various treatment groups was assessed by using two-tailed Student's t test or one- or two-way ANOVA, followed by Bonferroni posthoc comparison.

Materials and methods used for histological, confocal immu-nohistochemical, and transmission electron microscopic (TEM) studies, real-time quantitative RT-PCR assays of intestinal gene expression, and the administration of various neutralizing antibodies to recipient mice before TBI are described in *Supporting Materials and Methods* and Table 1, which are published as supporting information on the PNAS web site.

Results and Discussion

The Small Intestine of GF Mice Is Radioresistant. In most mouse strains, TBI ultimately causes death in CONV-R animals by bone marrow failure at doses of 10 Gy and death from a combination of bone marrow failure and radiation enteritis at doses ≥15 Gy. We developed protocols for exposing 8- to 12-week-old male and female GF FVB/N mice to TBI in a ^{137}Cs irradiator without compromising their GF status (see *Materials and Methods*). Age- and gender-matched GF and CONV-R mice were fed the same autoclaved chow diet and treated with identical levels of irradiation. To rescue the animals from death due to bone marrow failure, BMT was performed by retroorbital injection of antibiotic-sterilized unfractionated marrow harvested from age-, gender-, and strain-matched CONV-R donors. To confirm the efficacy of retroorbital delivery of bone marrow, control animals were transplanted after 10 Gy of TBI: >95% of GF and CONV-R mice (n = 23) survived ≥60 d, and all GF mice remained sterile as judged by periodic culture of their stool (and cecal contents at the time of being killed).

All GF mice treated with a higher TBI dose (16 Gy) followed by BMT survived for ≥40 d (n = 18). The GF mice ultimately succumbed to dental malocclusion due to the deleterious effects of irradiation on growth of the tooth bud. In contrast, 52% of CONV-R mice treated with 16 Gy followed by BMT died within 7 d (n = 27; P < 0.001, compared with GF; see Fig. 5A, which is published as supporting information on the PNAS web site). The role of the microbiota in imparting this increased radiosensitivity was confirmed by colonizing GF mice for 14 d with a cecal microbiota harvested from CONV-R donors. When the resulting CONV-D mice were treated with 16 Gy of TBI followed by BMT, 44% died within 7 d (n = 25, P < 0.005, compared with GF; no significant difference, compared with CONV-R animals; P = 0.40). A 14-d colonization of GF mice with *Bacteroides thetaiotaomicron* (sequenced strain VPI-5482) and/or *Escherichia coli* (sequenced strain MG1655), representing prominent obligate and facultative anaerobes, respectively, in the normal human and mouse microbiotas, did not affect their radioresistant phenotype after 16 Gy of TBI, even though the density of their colonization was similar to that achieved after conventionalization with a complete cecal microbiota from CONV-R donors (10^{11} to 10^{12} colony-forming units/ml cecal contents; n = 8 biassociated and 4 monoassociated mice). This result indicated that there is microbial specificity to the lethal radiosensitive phenotype imparted by the microbiota, and that one or more other species are required in lieu of, or in addition to, these two.

We performed a histological analysis to determine whether the different survival times of GF and colonized mice were due to a differential response of their small intestines to 16 Gy of TBI. GF FVB/N mice killed up to 14 d after TBI-BMT had no histological evidence of radiation enteritis (Fig. 5B). In contrast, their CONV-R or CONV-D counterparts had the classical hallmarks of this injury response when they were killed immediately after becoming moribund 5–7 d after TBI, whether or not they had received a BMT (n = 5–8 mice per group; Fig. 5C). The relative radioresistance of GF, compared with CONV-D or CONV-R intestines, disappeared at 20 Gy: all GF animals receiving this dose succumbed by 9 d after TBI–BMT with radiation enteritis (n = 8; data not shown).

CONV-R and CONV-D mice that received 14 Gy (a lethal TBI dose just below the threshold for developing radiation enteritis) and those that received 16 Gy (above the threshold)

MEDICAL SCIENCES

had no statistically significant differences in the mean number of aerobic or anaerobic bacteria in their spleens (5×10^6 colony-forming units per spleen at the lower dose vs. 1.3×10^7 colony-forming units per spleen at the higher dose; $n = 5$ mice per treatment group; $P = 0.49$ by using two-tailed Student's t test; nonirradiated controls had ≤ 10 colony-forming units per spleen). Thus, radiation-induced systemic infection is not sufficient to produce the histologic features of radiation enteritis.

Bone marrow from *Tie2-GFP* donors (transgene expression marks mucosal endothelial cells; ref. 26) or *Sca-1-EGFP* knock-in donors (locus marks all hematopoietic derivatives plus endothelial cells; ref. 27 and Fig. 6A, which is published as supporting information on the PNAS web site) was transplanted into GF, CONV-D, or CONV-R recipients treated with a dose of TBI that does not produce radiation enteritis (10 Gy). Six or 12 weeks later, very few GFP$^+$ cells were observed in the villus core mesenchyme of syngeneic recipient mice that received bone marrow from *Tie2-GFP* donors (data not shown). Irradiated recipients of bone marrow from *Sca1-EGFP* donors also did not have detectable GFP$^+$ endothelial cells in their villus core mesenchyme (Fig. 6B). However, there was extensive population of this mesenchyme with GFP$^+$/CD45$^+$ cells (CD45 is panleukocyte marker), as well as GFP$^+$/B220$^+$ B cells and GFP$^+$/CD3$^+$ T cells (Fig. 6C and data not shown).

Based on these findings, we concluded that (*i*) mice harboring a normal microbiota exhibit enhanced intestinal radiosensitivity, compared with GF animals, and that this enteritis is responsible for their increased mortality after TBI–BMT; (*ii*) BMT cannot rescue lethality due to radiation enteritis; and (*iii*) indigenous microbes alter the radioresponsive phenotype of the intestine independent of systemic infection or functions that are provided by transplanted, bone marrow-derived, villus mesenchymal cells.

The Microbiota Increases the Sensitivity of Mesenchymal Endothelial and Immune Cells to TBI-Induced Apoptosis. To further define differences in the radiosensitivity between GF and colonized mice, GF, CONV-D, and CONV-R FVB/N animals were treated with 16 Gy of TBI and killed 4 h later, and apoptotic (TUNEL$^+$) cells were scored in cryosections prepared from their distal small intestines ($n = 4$–5 mice per treatment group). The crypts of Lieberkühn, which contain the multipotential small intestinal stem cell and its differentiating descendants (oligopotential lineage progenitors and a transit-amplifying population), exhibited extensive epithelial apoptosis in all three groups of mice, as did cells in the mesenchymal cores of small intestinal villi in CONV-R and CONV-D animals (Fig. 1). In contrast, the number of apoptotic cells (i.e., those having TUNEL$^+$, DAPI-stained nuclei) in the mesenchymal cores of GF mice was significantly less (Fig. 1). Consistent with their post-TBI–BMT survival curves, there were no significant quantitative differences in the mesenchymal apoptotic response after 16 Gy of TBI in GF vs. *B. thetaiotaomicron*/*E. coli*-biassociated mice (Fig. 1D).

Time-course studies involving conventionalization of GF mice for 1, 2, 7, and 14 d before 16 Gy of TBI–BMT revealed that there were no significant differences in the number of TUNEL$^+$/DAPI$^+$ mesenchymal cells per villus section, compared with nonirradiated GF controls, until 14 d ($n = 3$ mice assayed per treatment group per time point). Administering considerably higher doses of TBI (22 Gy) to GF animals before TBI, or varying the interval between 16 Gy of TBI and their time of being killed from 1 to 24 h, did not yield a statistically significant increase in the number of apoptotic mesenchymal cells (data not shown). The development of radiation enteritis in GF mice in the absence of a significant mesenchymal apoptotic response 4 h after 22 Gy of TBI is consistent with the notion, gleaned from previous studies of CONV-R mice, that mesenchyme-
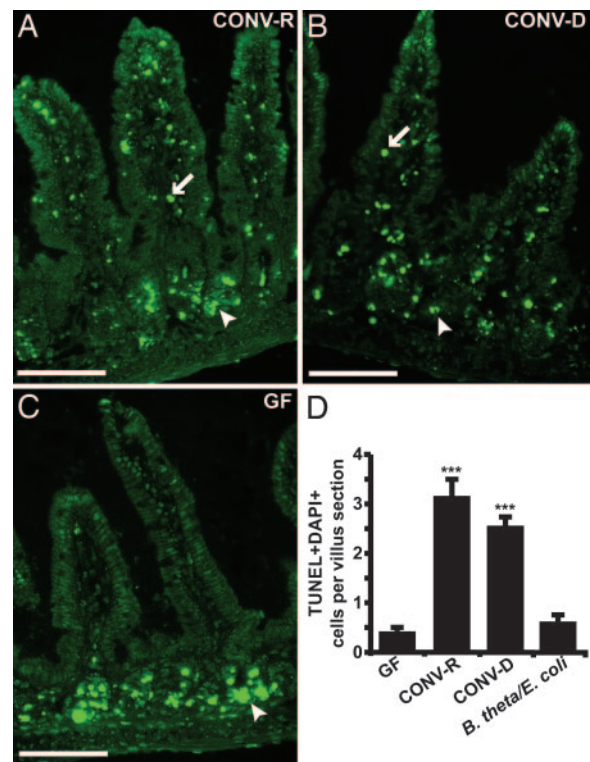
Fig. 1. Microbiota-associated sensitivity of villus core mesenchymal cells to TBI-induced apoptosis. TUNEL$^+$ cells appearing 4 h after 16 Gy of TBI in the distal small intestines of CONV-R (*A*), CONV-D (*B*), and GF (*C*) WT FVB/N mice. Fluorescence microscopy reveals green TUNEL$^+$ cells in the crypt epithelium (arrowheads) of all three mice and in the villus core mesenchyme (arrows) of CONV-R and CONV-D mice. In contrast, TUNEL$^+$ cells are absent from the villus core mesenchyme of the GF animal. (Scale bars, 50 μm.) (*D*) The mean number (± 1 SD) of TUNEL$^+$/DAPI$^+$ mesenchymal cells per distal small intestinal villus sections prepared from GF, CONV-R, CONV-D, and *B. theta*/*E. coli*-biassociated FVB/N mice (four to five mice scored per group; ≥ 100 villus sections assayed per animal). ∗∗∗, $P < 0.001$, compared with GF. In nonirradiated CONV-R controls, the mean number of apoptotic cells per section of villus core mesenchyme was ≤ 0.2.

independent, epithelial-based mechanisms underlie mucosal injury at these exceptionally high doses (28, 29).

Light microscopic multilabel immunohistochemical analysis using antibodies specific for CD31 (PECAM-1), and TEM studies, established that endothelial cells comprise a subset of the apoptotic villus mesenchymal population that appears in CONV-R mice 4 h after 16 of Gy TBI (Fig. 2 *A* and *B*). In contrast, endothelial cells in the villus mesenchyme of treatment-matched GF mice had normal ultrastructural morphology (Fig. 2C; $n \geq 30$ villus sections surveyed by TEM per animal, corresponding to ≥ 200 endothelial cells).

Administering 16 Gy of TBI to WT CONV-R and CONV-D mice also increased the number of CD45$^+$ apoptotic cells in the mesenchyme (Fig. 2D). Many of these cells were lymphocytes, judging by their reaction with antibodies to B220 or CD3 (data not shown).

Recent studies of CONV-R mice showed that progression to radiation enteritis correlates with radiation-induced endothelial apoptosis (28, 30). Our *in vivo* studies of gnotobiotic mice link the microbiota to both radiation enteritis and intestinal endothelial apoptosis. This linkage raises two important questions: Does the microbiota-associated enhancement of TBI-induced endothelial apoptosis require lymphocytes? What microbiota-regulated host genes impart resistance to TBI-induced endothelial cell apoptosis in GF mice?

Fig. 2. Apoptosis of CD31$^+$ endothelial cells and CD45$^+$ leukocytes in the villus mesenchyme of a CONV-R mouse treated with 16 Gy of TBI. (*A*) Small intestinal villus section stained with hematoxylin and eosin (*Left*). (Scale bar, 100 μm.) The expanded views of the boxed region (*Right*) show an adjacent section after staining with TUNEL reagents and antibodies to CD31. The arrow points to a TUNEL$^+$ nucleus in a CD31$^+$ endothelial cell. (Scale bar, 10 μm.) (*B*) TEM image of a mesenchymal endothelial cell (arrowhead) from the distal small intestine of a CONV-R mouse 4 h after 16 Gy of TBI. Nuclear condensation and cellular protrusion into the capillary lumen are characteristics of endothelial apoptosis. (Scale bar, 2 μm.) (*C*) A TEM image of a representative villus mesenchymal endothelial cell (arrowhead) from the distal small intestine of a GF B6 mouse killed 4 h after 16 Gy TBI. The cell has normal morphology. Epi, epithelium; Mes, mesenchyme, bb, brush border on the apical surface of enterocytes. (Scale bar, 4 μm.) (*D*) A single image from a 3D reconstruction of serial 1-μm-thick scans of a villus section from a CONV-R mouse killed 4 h after 16 Gy of TBI. Arrows denote TUNEL$^+$ CD45$^+$ cells, whereas arrowheads denote TUNEL$^+$ CD45$^-$ cells. CD45 is a surface marker, whereas TUNEL stains nuclei: therefore, TUNEL$^+$ cells that coexpress CD45 will not appear yellow. (Scale bar, 80 μm.) (*Inset*) A higher-power view of the boxed area.

A 14-d conventionalization of GF B6 *Rag1*$^{-/-}$ mice that lack mature lymphocytes, followed by 16 Gy of TBI, produced a statistically significant increase in mesenchymal cell death, compared with irradiated GF *Rag1*$^{-/-}$ controls (Fig. 3*A*). Nevertheless, these CONV-D B6 *Rag1*$^{-/-}$ mice had significantly fewer villus mesenchymal apoptotic cells than did age- and treatment-matched WT B6 animals ($n = 4$–6 mice per grou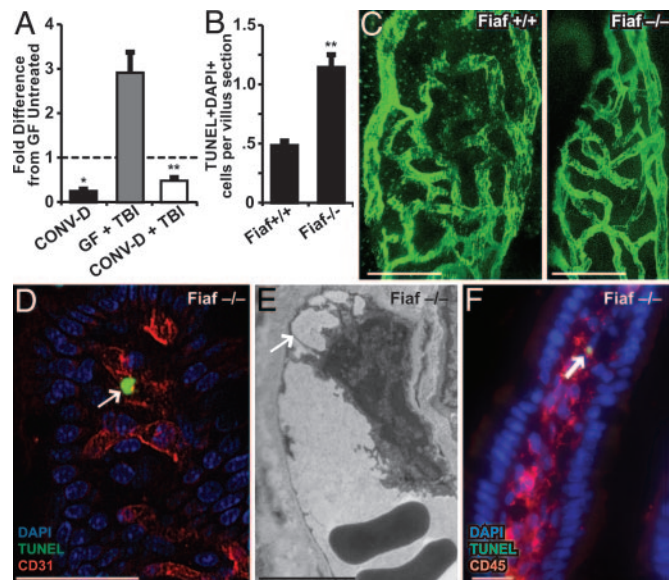p; Fig. 3*A*). Apoptotic CD31$^+$ endothelial cells as well as CD45$^+$ leukocytes were observed in the villus mesenchymal cores of these CONV-D *Rag1*$^{-/-}$ mice (Fig. 3 *B* and *C*), just as they were in irradiated CONV-D WT littermates. The differences in mesenchymal apoptosis between CONV-D *Rag1* knockout and WT animals were not attributable to differences in the complexity of the capillary network that underlies their small intestinal villus mucosa: i.v. injection of FITC-labeled *Bandeiraea simplicifolia*-1 lectin, which binds endothelial cells, followed by confocal microcopy and 3D reconstruction of serial digital images (see *Supporting Materials and Methods*), revealed no appreciable differences in vascular phenotypes between the two groups of animals (Fig. 3*D*).

Taken together, these results demonstrate that (*i*) lymphocytes comprise a portion of the villus mesenchymal population of TBI-induced apoptotic cells in WT mice with a microbiota; (*ii*) a subset of the CD45$^+$ cells that populate the villus mesenchyme of CONV-D *Rag1*$^{-/-}$ mice is sensitive to TBI-induced apoptosis; and (*iii*) mature B and T cells are not required for induction of endothelial apoptosis.

We extended these studies by administering 16 Gy of TBI to CONV-D B6 WT and *Rag1*$^{-/-}$ littermates, followed by BMT with genotype and gender-matched marrow. All mice in each conventionalized group died within 7 d after TBI–BMT and exhibited histologic evidence of radiation enteritis ($n = 8$–10 mice per group; data not shown). This result indicates that the microbiota can confer sensitivity to lethal radiation enteritis in animals that lack mature lymphocytes.

Fasting-Induced Adipose Factor (Fiaf) Conveys Radioresistance to Villus Endothelial Cells in GF Mice. Fiaf (also known as angiopoietin-like protein 4) is predicted to be composed of coil-coiled and fibrinogen-like domains; it is known to be glycosylated, proteolytically processed, and secreted from several mouse tissues, including the intestinal epithelium (31–34). *Fiaf* expression is selectively and significantly down-regulated in the gut epithelium by conventionalization of B6 GF mice (4.4- $\pm$ 0.5-fold; $n = 4$ mice per group; $P < 0.05$; Fig. 4*A* and ref. 3). This down-regulation is an evolutionarily conserved response, e.g., it occurs during the conventionalization of GF zebrafish (35). Fiaf is a physiologically important circulating inhibitor of lipoprotein lipase, and studies of GF and CONV-D WT and *Fiaf*$^{-/-}$ mice indicate that Fiaf is a key mediator of the microbiota's ability to promote host storage of energy, extracted from otherwise indigestible dietary polysaccharides, in adipocytes (3). Intriguingly, Fiaf also supports endothelial survival (31) and vascular sprouting *in vitro* (36) through unknown mechanisms. Given its suppression in the gut epithelium by the microbiota, we used *Fiaf*$^{-/-}$ mice to determine whether this protein plays a role in imparting radioresistance to villus core mesenchymal endothelial cells in GF animals.

Four hours after 18 Gy of TBI, the number of TUNEL$^+$/DAPI$^+$ mesenchymal cells per villus section was 2.4 $\pm$ 0.2-fold greater in 6- to 10-week-old GF *Fiaf*$^{-/-}$ mice, compared with their treatment-matched WT littermates ($P < 0.01$; $n = 9$ mice per group; Fig. 4*B*). Immunohistochemical and TEM analyses confirmed the presence of CD31$^+$ and CD45$^+$ apoptotic cells in the small intestinal mesenchyme of these irradiated GF *Fiaf*$^{-/-}$ mice (e.g., Fig. 4 *D*–*F*). This difference was not attributable to differences in the complexity of their submucosal villus capillary network: network density was similar in untreated GF knockout and WT animals (Fig. 4*C*).

The reduced expression of *Fiaf* produced by a 14-d conventionalization of GF WT mice also is evident 4 h after 16 Gy of TBI ($n = 4$ mice per group, $P < 0.01$; Fig. 4*A*). Thus, in the

Fig. 3. $Rag1^{-/-}$ mice reveal that the microbiota-dependent apoptotic response of villus endothelial cells to 16 Gy of TBI does not require mature T or B cells. (*A*) Quantitative assessment of TUNEL$^+$ DAPI$^+$ cells in the villus mesenchyme of B6 GF and CONV-D WT and $Rag1^{-/-}$ mice killed 4 h after 16 Gy of TBI ($n = 4–6$ mice per group; $\geq$100 villus sections assayed per mouse). ***, $P <$ 0.001, compared with GF $Rag1^{+/+}$ mice; **, $P <$ 0.01, compared with GF $Rag1^{-/-}$ mice; Ψ, $P <$ 0.05, compared with CONV-D $Rag1^{+/+}$ mice. (*B*) Two TUNEL$^+$ CD31$^+$ endothelial cells (arrows) in the small intestinal villus mesenchyme of a CONV-D $Rag1^{-/-}$ mouse treated as in *A*. The image was acquired from a 0.5-μm-thick digital scan of the section. (*C*) Adjacent section showing two TUNEL$^+$ CD45$^+$ leukocytes (arrows) in the villus mesenchyme. (*D*) Microscopic angiograms showing single images from 3D reconstructions of serial 1-μm-thick scans of nonirradiated distal small intestinal villi from CONV-D $Rag1^{+/+}$ and $Rag1^{-/-}$ distal small intestinal villi. The complexity of the submucosal capillary network present in the villus core mesenchyme can be assessed by noting the size of open areas ("windows") circumscribed by interconnected vessels. Analysis of this parameter indicated that network complexity was not appreciably different between $Rag1^{-/-}$ and WT mice with the two genotypes. (Scale bars, 20 μm.)

Fig. 4. Loss of Fiaf results in loss of resistance to TBI-induced apoptosis in GF mice. (*A*) Quantitative RT-PCR analysis shows that conventionalization of GF WT mice suppresses Fiaf expression in the distal small intestine and that this effect is not abrogated after 16 Gy of TBI (mean values $\pm$ 1 SD are plotted; $n =$ 4 mice per group; *, $P <$ 0.05, compared with GF untreated B6 mice; **, $P <$ 0.01, compared with GF mice treated with 16 Gy of TBI 4 h before they were killed). (*B*) Quantitative assessment of apoptosis in the villus mesenchyme of GF $Fiaf^{-/-}$ mice and their WT littermates 4 h after 18 Gy of TBI ($n = 9$ mice per group; $\geq$100 villus sections assayed per mouse; mean $\pm$ 1 SD; **, $P <$ 0.01, compared with GF $Fiaf^{+/+}$). (*C*) Single images from digital 3D reconstructions of small intestinal villus capillary networks in GF $Fiaf^{-/-}$ and their WT littermates. (Scale bars, 20 μm.) (*D*) TUNEL$^+$ CD31$^+$ endothelial cell (arrow) in the small intestinal villus mesenchyme of a GF $Fiaf^{-/-}$ mouse treated as in *A*. (Scale bar, 50 μm.) (*E*) TEM image of a villus mesenchymal endothelial cell in a $Fiaf^{-/-}$ mouse killed 4 h after 18 Gy of TBI. Note the nuclear protrusion and avulsion from the basement membrane (arrow), two ultrastructural manifestations of endothelial cell death. (Scale bar, 5 μm.) (*F*) TUNEL$^+$ CD45$^+$ leukocyte (arrow) in the small intestinal villus mesenchyme of a GF $Fiaf^{-/-}$ mouse treated as in *A*. (Scale bar, 20 μm.)

colonized state, Fiaf has a minimized capacity to provide radioprotection to endothelial cells and lymphocytes in WT mice: this would explain why Fiaf affords radioprotection in GF WT mice (there is no microbial suppression of its production) and why there was no significant difference in the magnitude of TBI-induced mesenchymal apoptosis between CONV-D WT mice (Fiaf suppressed state) and their CONV-D $Fiaf^{-/-}$ littermates (data not shown).

GF $Fiaf^{-/-}$ mice do not display an increased likelihood for developing lethal radiation enteritis, compared with GF WT littermates, as judged by histological studies and the absence of differences in the survival curves of animals given 16–18 Gy of TBI, followed by gender- and genotype-matched BMT ($n =$ 10 animals per group; data not shown). This finding suggests that other factors operate in collaboration with or independent of Fiaf to convey these phenotypes. Inducible nitric oxide synthase (iNOS) does not appear to be one of these factors. Nitric oxide is a known regulator of endothelial survival: at

nanomolar concentrations, it is cytoprotective, whereas at micromolar concentrations (achieved with inflammatory stimuli), it is cytotoxic (37, 38). Quantitative RT-PCR analysis indicated that 4 h after 16 Gy of TBI, iNOS mRNA levels are higher (8.5- $\pm$ 1.9-fold) in the distal small intestines of 8-week-old B6 WT CONV-D mice, compared with their GF counterparts ($n = 4$ mice per group; $P <$ 0.001). Fiaf deficiency does not affect the magnitude of these TBI-induced differences in *iNOS* expression (data not shown). Moreover, our analysis of CONV-R $iNOS^{-/-}$ mice revealed that loss of this nitric oxide-producing enzyme had no detectable effect on the extent of villus mesenchymal apoptosis produced by 16 Gy of TBI ($n = 7$ mice per group; data not shown).

Pharmacologic and genetic studies have revealed that three other factors modulate the intestine's mesenchymal apoptotic response to γ-irradiation. Administration of FGF-2 decreases TBI-associated mortality and attenuates TBI-induced intestinal mesenchymal apoptosis in CONV-R WT mice (28, 39). Pretreatment with VEGF-A provides partial protection against lethal radiation enteritis (39). CONV-R mice homozygous for a null allele of the gene encoding acid sphingomyelinase (ASMase) have reduced TBI-induced gut mesenchymal apoptosis and lethality, compared with their CONV-R WT littermates (28). However, quantitative RT-PCR studies of GF and CONV-D WT and Fiaf-knockout mice before and 4 h after 16 Gy of TBI revealed that conventionalization, TBI, and Fiaf

deficiency do not produce a significant effect on the levels of small intestinal expression of FGF-2, VEGF-A, or ASMase mRNAs ($n = 4$ mice per group; data not shown). Moreover, when we administered a well characterized neutralizing antibody to mouse VEGF-A, at doses known to block the effects of this protein in *in vivo* angiogenesis assays (40–43), no discernable difference in the extent of TBI-induced mesenchymal cell death was detected (reference control, WT GF mice injected with control IgG antibody; $n = 6$ mice per group; data not shown). In addition, administration of well characterized neutralizing antibodies against FGF-2, at a dose known to affect postnatal coronary angiogenesis *in vivo* (41), did not affect (enhance) the levels of mesenchymal cell death in irradiated GF WT mice, compared with animals treated with an analogous Ig control ($n = 4$ mice per group, data not shown). Together, these latter findings suggest that VEGF-A and FGF-2 are not essential for Fiaf-mediated radioprotection in GF mice.

Prospectus. The ability to administer TBI, followed by transplantation of normal or genetically manipulated bone marrow to normal or genetically manipulated GF mice, has revealed (*i*) the importance of the microbiota in conveying radiosensitivity to the small intestinal endothelium, (*ii*) the absence of a requirement for mature lymphocytes in conveying this microbiota-induced radiosensitive phenotype, and (*iii*) the contributions of Fiaf, a microbiota-regulated, epithelial-derived, secreted protein, to radioresistance. GF *Fiaf*$^{-/-}$ mice provide an opportunity to conduct further proof-of-principle tests of whether Fiaf or its proteolytically processed derivatives (33, 34), whether administered via transgenes that are not suppressed in the gut epithelium by the microbiota or as injected purified polypeptides, can function as therapeutically useful gut radioprotective agents. These mice also provide an opportunity to further assess the signaling pathways through which the microbiota and Fiaf operate to regulate endothelial cell biology. Finally, the methods described in this report for producing gnotobiotic chimeric mice by using sterilized marrow from CONV-R normal or genetically manipulated donors and irradiated GF recipients provides a potentially versatile approach for characterizing cellular and/or molecular factors that participate in the cross-talk between elements of the microbiota, the host epithelium, and the immune system.

1. Eckburg, P. B., Bik, E. M., Bernstein, C. N., Purdom, E., Dethlefsen, L., Sargent, M., Gill, S. R., Nelson, K. E. & Relman, D. A. (2005) *Science* **308,** 1635–1638.
2. Bäckhed, F., Ley, R. E., Sonnenburg, J. L., Peterson, D. A. & Gordon, J. I. (2005) *Science* **307,** 1915–1920.
3. Bäckhed, F., Ding, H., Wang, T., Hooper, L. V., Koh, G. Y., Nagy, A., Semenkovich, C. F. & Gordon, J. I. (2004) *Proc. Natl. Acad. Sci. USA* **101,** 15718–15723.
4. Savage, D. C. (1986) *Annu. Rev. Nutr.* **6,** 155–178.
5. Hooper, L. V., Midtvedt, T. & Gordon, J. I. (2002) *Annu. Rev. Nutr.* **22,** 283–307.
6. Krul, C., Humblot, C., Philippe, C., Vermeulen, M., van Nuenen, M., Havenaar, R. & Rabot, S. (2002) *Carcinogenesis* **23,** 1009–1016.
7. Humblot, C., Lhoste, E., Knasmuller, S., Gloux, K., Bruneau, A., Bensaada, M., Durao, J., Rabot, S., Andrieux, C. & Kassie, F. (2004) *J. Chromatogr.* **802,** 231–237.
8. Abrams, G. D., Bauer, H. & Sprinz, H. (1963) *Lab. Invest.* **12,** 355–364.
9. Lesher, S., Walburg, H. E., Jr., & Sacher, G. A., Jr. (1964) *Nature* **202,** 884–886.
10. Khoury, K. A., Floch, M. H. & Hersh, T. (1969) *J. Exp. Med.* **130,** 659–670.
11. Savage, D. C., Siegel, J. E., Snellen, J. E. & Whitt, D. D. (1981) *Appl. Environ. Microbiol.* **42,** 996–1001.
12. Macpherson, A. J. & Uhr, T. (2004) *Science* **303,** 1662–1665.
13. Macdonald, T. T. & Monteleone, G. (2005) *Science* **307,** 1920–1925.
14. Stappenbeck, T. S., Hooper, L. V. & Gordon, J. I. (2002) *Proc. Natl. Acad. Sci. USA* **99,** 15451–15455.
15. Somosy, Z., Horvath, G., Telbisz, A., Rez, G. & Palfia, Z. (2002) *Micron* **33,** 167–178.
16. Livstone, E. M., Hersh, T., Spiro, H. M. & Floch, M. H. (1970) *Yale J. Biol. Med.* **42,** 448–454.
17. Brook, I., Walker, R. I. & MacVittie, T. J. (1988) *Int. J. Radiat. Biol. Relat. Stud. Phys. Chem. Med.* **53,** 709–716.
18. Brook, I. & Ledney, G. D. (1992) *Radiat. Res.* **130,** 61–64.
19. Reyniers, J. A., Trexler, P. C., Scruggs, W., Wagner, M. & Gordon, H. A. (1956) *Radiat. Res.* **5,** 591.
20. McLaughlin, M. M., Dacquisto, M. P., Jacobus, D. P. & Horowitz, R. E. (1964) *Radiat Res.* **23,** 333–349.
21. Matsuzawa, T. (1965) *Tohoku J. Exp. Med.* **85,** 257–263.
22. Onoue, M., Uchida, K., Yokokura, T., Takahashi, T. & Mutai, M. (1981) *Radiat. Res.* **88,** 533–541.
23. Wilson, R. (1968) *J. Am. Osteopath. Assoc.* **67,** 653–662.
24. Heit, H., Fliedner, T. M., Fache, I. & Schnell, G. (1970) *Radiat. Res.* **41,** 163–182.
25. Hooper, L. V., Mills, J. C., Roth, K. A., Stappenbeck, T. S., Wong, M. H. & Gordon, J. I. (2002) in *Molecular Cellular Microbiology*, eds. Sansonetti, P. & Zychlinsky, A. (Academic, San Diego), Vol. 31, pp. 559–589.
26. Motoike, T., Loughna, S., Perens, E., Roman, B. L., Liao, W., Chau, T. C., Richardson, C. D., Kawate, T., Kuno, J., Weinstein, B. M., *et al.* (2000) *Genesis* **28,** 75–81.
27. Hanson, P., Mathews, V., Marrus, S. H. & Graubert, T. A. (2003) *Exp. Hematol. (Charlottesville, Va.)* **31,** 159–167.
28. Paris, F., Fuks, Z., Kang, A., Capodieci, P., Juan, G., Ehleiter, D., Haimovitz-Friedman, A., Cordon-Cardo, C. & Kolesnick, R. (2001) *Science* **293,** 293–297.
29. Ch'ang, H.-J., Maj, J. G., Paris, F., Xing, H. R., Zhang, J., Truman, J.-P., Cardon-Cardo, C., Haimovitz-Friedman, A., Kolesnick, R. & Fuks, Z. (2005) *Nat. Med.* **11,** 484–490.
30. Cho, C.-H., Kammerer, R. A., Lee, H. J., Yasunaga, K., Kim, K.-T., Choi, H.-H., Kim, W., Kim, S.-H., Park, S. K., Lee, G.-M. & Koh, G.-Y. (2004) *Proc. Natl. Acad. Sci. USA* **101,** 5553–5558.
31. Kim, I., Kim, H. G., Kim, H., Kim, H. H., Park, S. K., Uhm, C. S., Lee, Z. H. & Koh, G. Y. (2000) *Biochem. J.* **346,** 603–610.
32. Mandard, S., Zandbergen, F., Tan, N. S., Escher, P., Patsouris, D., Koenig, W., Kleemann, R., Bakker, A., Veenman, F., Wahli, W., *et al.* (2004) *J. Biol. Chem.* **279,** 34411–34420.
33. Ge, H., Yang, G., Yu, X., Pourbahrami, T. & Li, C. (2004) *J. Lipid Res.* **45,** 2071–2079.
34. Ge, H., Yang, G., Huang, L., Motola, D. L., Pourbahrami, T. & Li, C. (2004) *J. Biol. Chem.* **279,** 2038–2045.
35. Rawls, J. F., Samuel, B. S. & Gordon, J. I. (2004) *Proc. Natl. Acad. Sci. USA* **101,** 4596–4601.
36. Le Jan, S., Amy, C., Cazes, A., Monnot, C., Lamande, N., Favier, J., Philippe, J., Sibony, M., Gasc, J. M., Corvol, P. & Germain, S. (2003) *Am. J. Pathol.* **162,** 1521–1528.
37. Chung, H. T., Pae, H. O., Choi, B. M., Billiar, T. R. & Kim, Y. M. (2001) *Biochem. Biophys. Res. Commun.* **282,** 1075–1079.
38. Walford, G. A., Moussignac, R. L., Scribner, A. W., Loscalzo, J. & Leopold, J. A. (2004) *J. Biol. Chem.* **279,** 4425–4432.
39. Okunieff, P., Mester, M., Wang, J., Maddox, T., Gong, X., Tang, D., Coffee, M. & Ding, I. (1998) *Radiat. Res.* **150,** 204–211.
40. Gorski, D. H., Beckett, M. A., Jaskowiak, N. T., Calvin, D. P., Mauceri, H. J., Salloum, R. M., Seetharam, S., Koons, A., Hari, D. M., Kufe, D. W. & Weichselbaum, R. R. (1999) *Cancer Res.* **59,** 3374–3378.
41. Tomanek, R. J., Sandra, A., Zheng, W., Brock, T., Bjercke, R. J. & Holifield, J. S. (2001) *Circ. Res.* **88,** 1135–1141.
42. Nakayama, T., Yao, L. & Tosato, G. (2004) *J. Clin. Invest.* **114,** 1317–1325.
43. Michel, F., Ambroisine, M. L., Duriez, M., Delcayre, C., Levy, B. I. & Silvestre, J. S. (2004) *Circulation* **109,** 1933–1937.

MEDICAL SCIENCES